

Supplementary Figure 1: *FGFR3*-altered bladder cancers shape a cold TME indirectly, related to Figure 1.

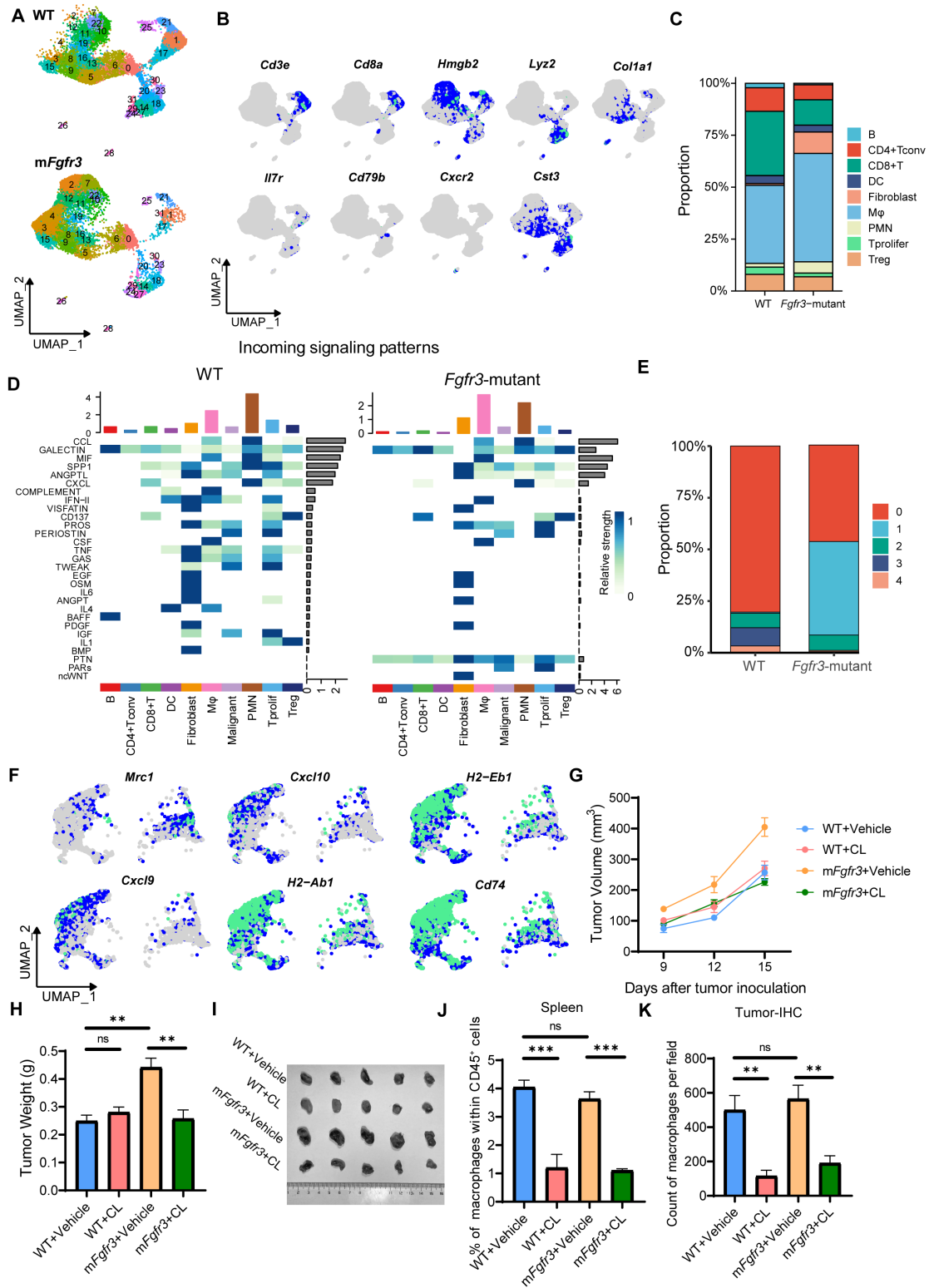
A, B, Picture of dissected tumors of the WT and *mFgfr3* tumors in the nude mice (**A**) and C57BL/6 mice (**B**).

C, Gating strategy for flow cytometry analysis on T cells in this study.

D, t-SNE plots show the landscape of infiltration of various types of T cells in the WT and *mFgfr3* tumors.

E, F, Schematic illustration shows the preparation of cancer supernatants-lymphocytes transwell assay (**E**) and the cancer cells-lymphocytes co-culture assay (**F**).

Scale bar: 1cm. (**E, F**: created with BioRender.com).



Supplementary Figure 2. scRNA-seq highlights the central role of macrophages in inducing the cold TME of the mFgfr3 tumor, related to Figure 2.

A, UMAP plot of single cells RNA sequencing results of WT and mFgfr3 MB49 mice tumors colored by clusters

B, FeaturePlots shows the expression of cluster-specific genes.

C, Stacked bar plot shows the proportion of each cell type in the WT and *mFgfr3* tumors.

D, Heatmap illustrates the level of incoming signaling to each cell type.

E, Stacked bar plot shows the proportion of each sub-cluster within macrophages in the WT and *mFgfr3* tumors.

F, FeaturePlots shows the expression of upregulated and downregulated genes in the sub-cluster 1 macrophages compared with other macrophages, left: macrophages from WT tumors; right: macrophages from *mFgfr3* tumors.

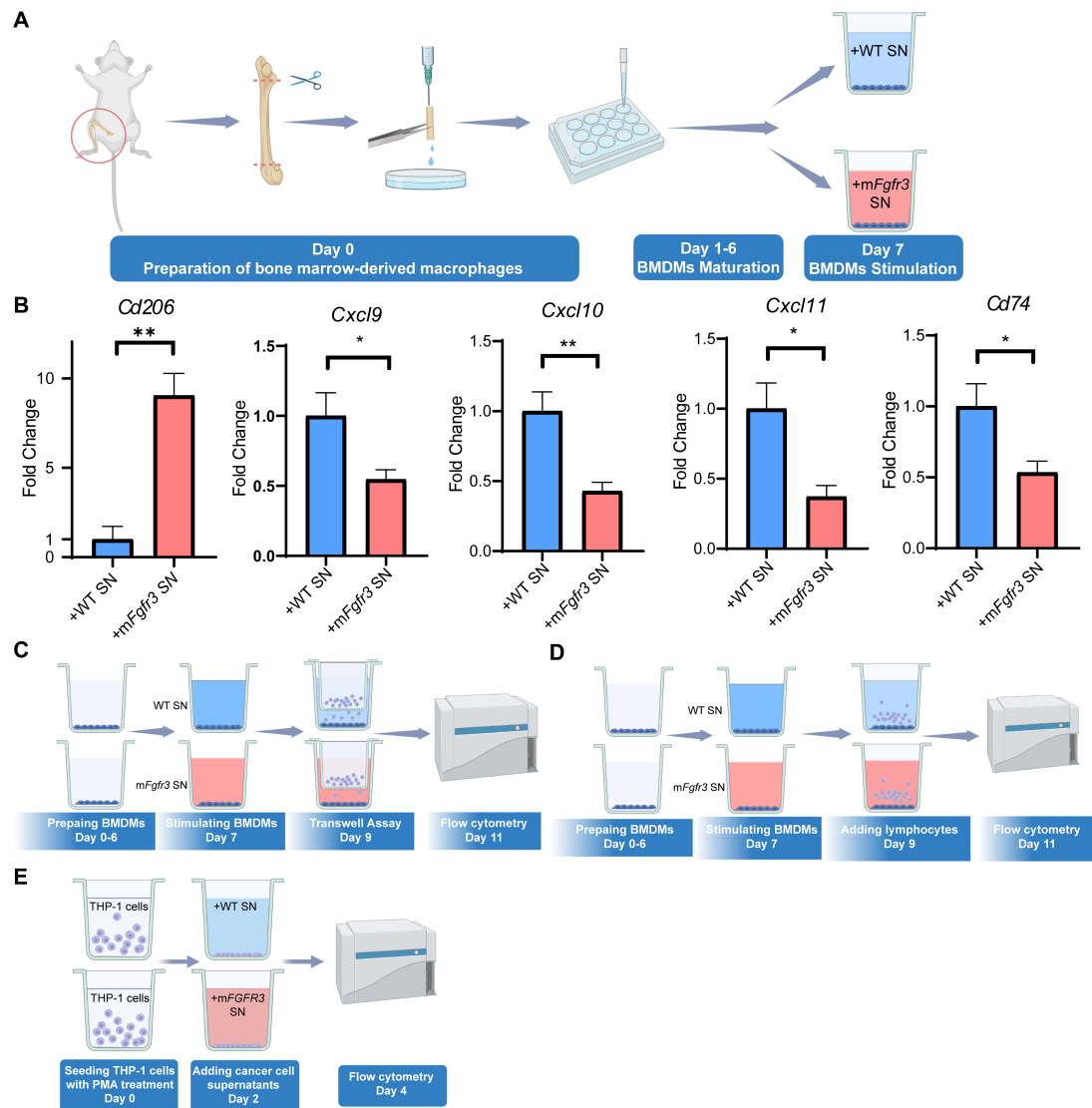
G, H, Growth curves (**G**) and tumor weights (**H**) of tumors in the indicated groups.

I, Picture of dissected tumors of the indicated groups.

J, Statistic analysis of the infiltration of macrophages in the spleens of the indicated group.

K, Statistic analysis of the infiltration of macrophages in the tumors of the indicated group

Error bars represent the mean \pm SEM. $p < 0.05$ was considered a significant difference, ns was no significance (one-way ANOVA with Holm-Sidak multiple comparison tests and unpaired parametric Student's t-test). * $p < 0.05$, ** $p < 0.01$, *** $p < 0.001$. M ϕ : Macrophages.



Supplementary Figure 3. *mFgfr3* cancer cells promote macrophage shift to an immune-inert phenotype, related to Figure 3.

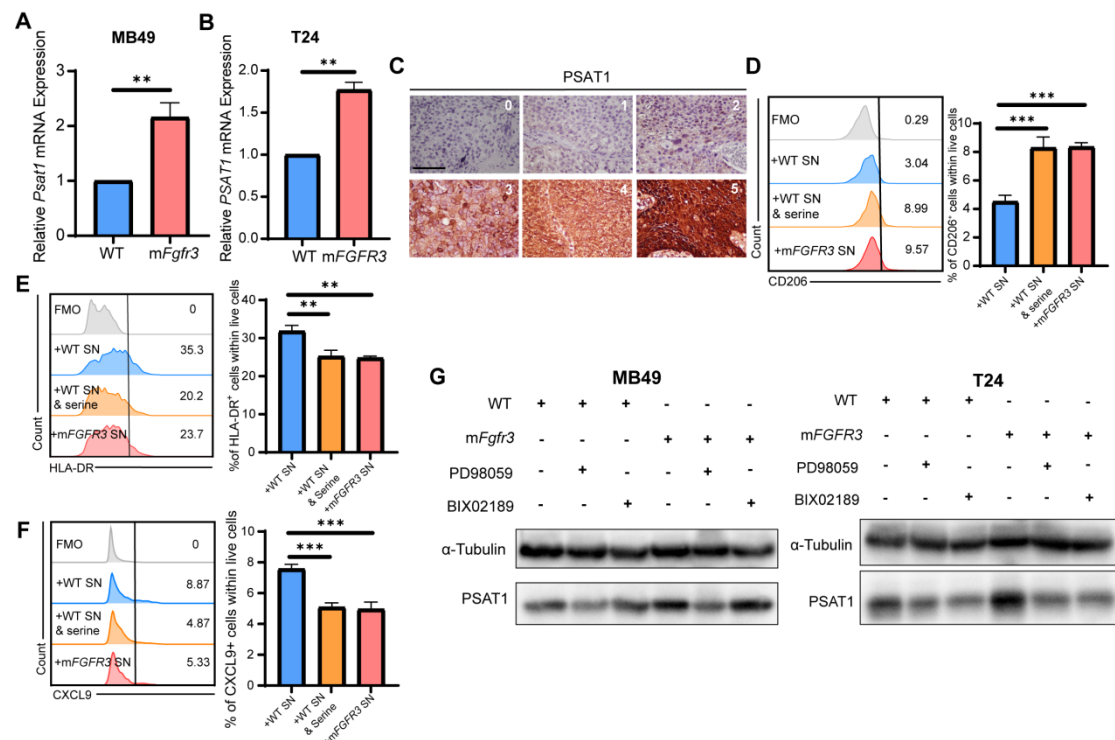
A, Schematic illustration of preparation and stimulation of the BMDMs.

B, Histograms show the qRT-PCR results of *Cd206*, *Cxcl9*, *Cxcl10*, *Cxcl11*, and *Cd74* expression in the macrophages stimulated with the WT and *mFgfr3* supernatants, $n = 3$.

C, **D**, Schematic illustration shows the preparation of the BMDMs-splenocytes transwell assay (**C**) and the *in vitro* BMDMs-splenocytes co-culture assay (**D**).

E, Schematic illustration of preparation, culturing, and stimulation of THP-1 cells, PMA: phorbol 12-myristate 13-acetate.

Error bars represent the mean \pm SEM. $p < 0.05$ was considered a significant difference, ns was no significance (unpaired parametric Student's t-test). * $p < 0.05$, ** $p < 0.01$. (**A**, **C**, **D**, **E**: created with BioRender.com).



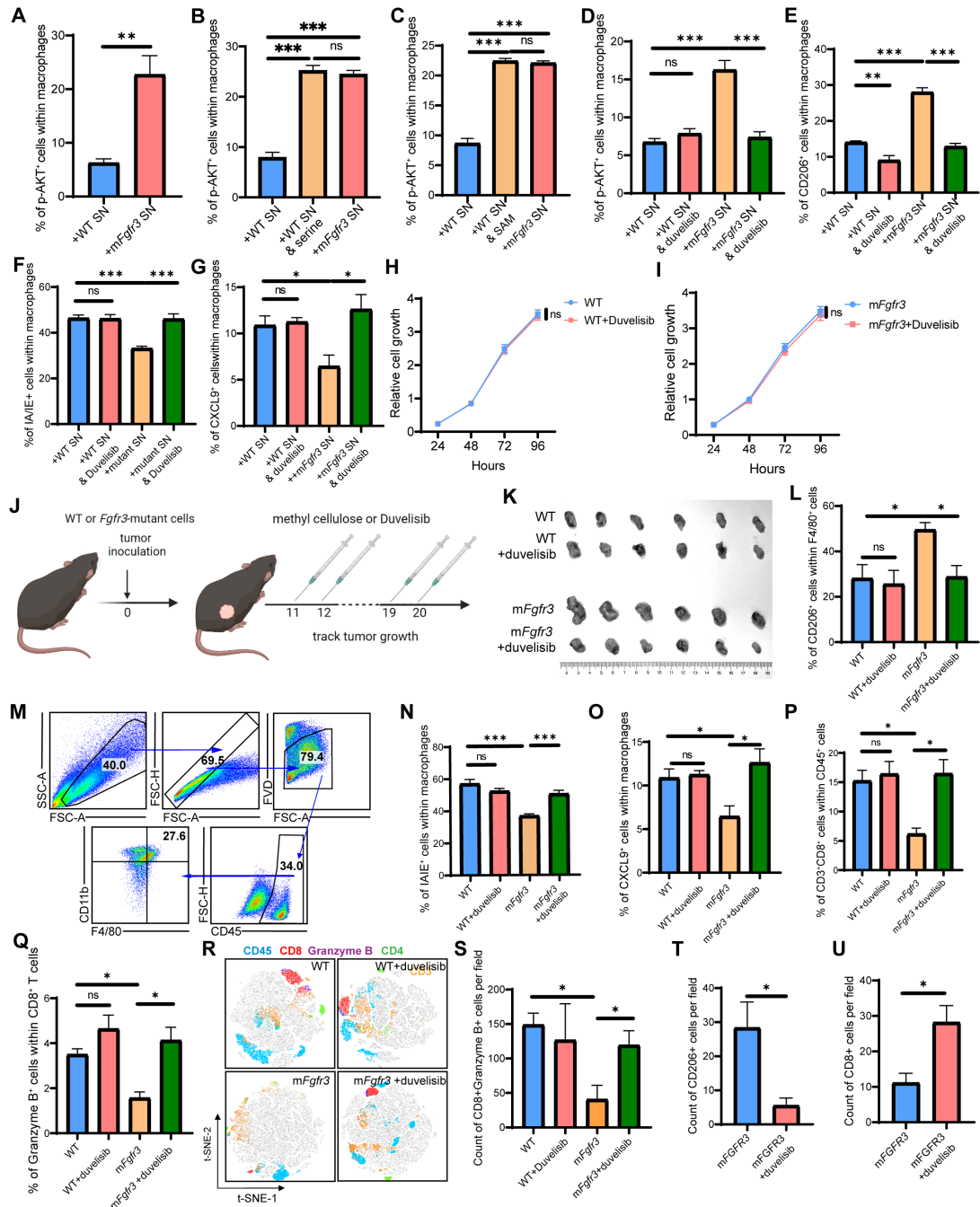
Supplementary Figure 4: *mFGFR3* cancer cells upregulate serine synthesis to shift macrophages to an immune-inert phenotype, related to Figure 4.

A, B, Statistic analysis of the qRT-PCR results shows the *Psat1* or *PSAT1* expression in the WT and mutant cancer cells.

C, Representative IHC pictures show different PSAT1 scores.

D, E, F, flow cytometry results and statistical analysis of the proportion of CD206⁺ cells (**D**), HLA-DR⁺ cells (**E**), and CXCL9⁺ cells (**F**) within macrophages in the indicated groups from the THP-1 cell stimulated with cancer cell supernatant experiment, *n* = 6.

G, Western blot analysis of the PSAT1 expression following supplementing the ERK1/2 inhibitor (PD98059) or ERK5 inhibitor (BIX02189) in the indicated groups. Error bars represent the mean ± SEM. *p* < 0.05 was considered a significant difference, ns was no significance (one-way ANOVA with Holm-Sidak multiple comparison tests and unpaired parametric Student's t-test). **p* < 0.05, ***p* < 0.01, ****p* < 0.001.



Supplementary Figure 5: Targeting the PI3K/Akt pathway in macrophages reverses macrophage phenotypes in *mFgfr3* cancers, related to Figure 5.

A, B, C, D, Statistical analysis of the proportion of p-AKT⁺ cells within macrophages in the indicated groups.

E, F, G, Statistical analysis of the proportion of CD206⁺ cells (**E**), IA/IE⁺ cells (**F**), and CXCL9⁺ cells (**G**) within macrophages in the indicated groups.

H, I, cell viability assays show the relative cell proliferation in the control group and duvelisib group on WT cells (**H**) and *mFgfr3* cells (**I**).

J, Schematic illustration shows the treatment plan of duvelisib in the WT and *mFgfr3*

tumors.

K, Picture of dissected tumors of the indicated groups in the duvelisib treatment experiment.

L, Statistical analysis illustrating the proportion of CD206⁺ cells within macrophages in the indicated groups.

M, Gating strategy for flow cytometry analysis on macrophages in this study.

N, O, Statistical analysis illustrating the proportion of IA/IE⁺ cells (**N**) and CXCL9⁺ cells (**O**) within macrophages in the indicated groups.

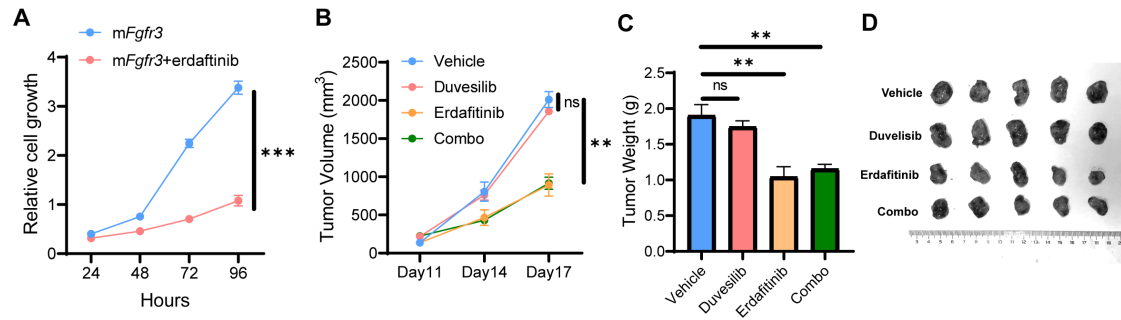
P, Q, Statistical analysis illustrating the proportion of CD3⁺CD8⁺ cells within CD45⁺ cells (**P**) and the proportion of Granzyme B⁺ cells within CD8⁺ T cells (**Q**) in the indicated groups.

R, t-SNE plots show the landscape of T cell infiltration in the indicated groups.

S, Statistical analysis illustrating the proportion of CD8⁺ Granzyme B⁺ cells in the indicated groups.

T, U, Statistical analysis illustrating the proportion of CD206⁺ cells (**T**) and CD8⁺ cells (**U**) in the indicated groups.

Error bars represent the mean \pm SEM. $p < 0.05$ was considered a significant difference, ns was no significance (one-way ANOVA with Holm-Sidak multiple comparison tests and unpaired parametric Student's t-test). * $p < 0.05$, ** $p < 0.01$, *** $p < 0.001$. (**J**: created with BioRender.com).



Supplementary Figure 6: Duvelisib augments the anti-tumor efficacy of erdafitinib in combination therapy, related to Figure 6.

A, cell viability assays show the relative cell proliferation in the control group and erdafitinib group on *mFgfr3* cells.

B, C, Growth curves (**B**) and tumor weights (**C**) of tumors in the indicated groups from the nude mice combination treatment experiment.

D, Picture of dissected tumors of the indicated groups from the nude mice combination treatment experiment.

Error bars represent the mean \pm SEM. $p < 0.05$ was considered a significant difference, ns was no significance (one-way ANOVA with Holm-Sidak multiple comparison tests and unpaired parametric Student's t-test). * $p < 0.05$, ** $p < 0.01$, *** $p < 0.001$.